

Unrolling SGD: Understanding Factors Influencing Machine Unlearning

Anvith Thudi^{†‡}, Gabriel Deza^{†‡}, Varun Chandrasekaran^{*}, Nicolas Papernot^{†‡}

[†]University of Toronto, [‡]Vector Institute, ^{*}University of Wisconsin-Madison

Abstract

Machine unlearning is the process through which a deployed machine learning model forgets about one of its training data points. While naively retraining the model from scratch is an option, it is almost always associated with a large computational effort for deep learning models. Thus, several approaches to *approximately unlearn* have been proposed along with corresponding metrics that formalize what it means for a model to forget about a data point. In this work, we first taxonomize approaches and metrics of approximate unlearning. As a result, we identify *verification error*, i.e., the ℓ_2 difference between the weights of an approximately unlearned and a naively retrained model, as a metric approximate unlearning should optimize for as it implies a large class of other metrics. We theoretically analyze the canonical stochastic gradient descent (SGD) training algorithm to surface the variables which are relevant to reducing the verification error of approximate unlearning for SGD. From this analysis, we first derive an easy-to-compute proxy for verification error (termed *unlearning error*). The analysis also informs the design of a new training objective penalty that limits the overall change in weights during SGD and as a result facilitates approximate unlearning with lower verification error. We validate our theoretical work through an empirical evaluation on CIFAR-10, CIFAR-100, and IMDB sentiment analysis.

1 Introduction

The goal of machine unlearning is to provide a mechanism for removing the impact a datapoint in the training set had on the final model. This is motivated by multiple settings where forgetting a datapoint is paramount. For example, a model which has not unlearned may leak some of the private information contained in a point [1, 2]. This is particularly relevant in scenarios where a particular user who owns the data later revokes access to it—a possibility popularized by the *right-to-be-forgotten* in the GDPR [3]. This possibility

of leakage is exacerbated by the ability of a ML model to memorize parts of its dataset [4, 5].

Machine unlearning was first introduced by Cao *et al.* [6] to unlearn datapoints for simple hypothesis spaces which have known SQ learning algorithms. Machine unlearning has since been extended to deep neural networks (DNNs) [7, 8, 9, 10, 11, 12, 13] where there are currently two broad approaches to machine unlearning: retraining and approximate unlearning.

With retraining, the point to be unlearned is removed from the training set, and a new model is trained from scratch on this updated training set. This approach has the advantage of carrying a strong claim for why the new model was not influenced in any way by the point to be unlearned, as it is not trained on it. This is a non-trivial advantage when unlearning needs to be transparent, e.g., in the context of right-to-be-forgotten requests [3]. Naively retraining from scratch can be made more efficient, as demonstrated by the SISA framework [7]. Nevertheless it is still an expensive process that requires changes to the training pipeline.

In approximate unlearning, the model owner instead starts from the existing model and seeks to modify its weights so as to obtain a slightly different model which satisfies an unlearning *criterion* (e.g., poor performance on the point to be unlearned, or *similar* weights to a model naively retrained without the point to be unlearned, etc). This can be done for example through a form of gradient ascent [8], which is the opposite of gradient descent performed to train the model normally. Alternatively various approaches suggest hessian-based updates [9, 11]. Approximate unlearning has the advantage of being more computationally efficient than retraining but comes at the expense of a weaker guarantee: the model learnt may not be completely uninfluenced by the unlearned datapoint.

Underlying the ambiguity with the various approximate claims to unlearning is simply the variety of such unlearning criterion that individual approaches consider and their associated metrics: each typically has their own merit to measuring unlearning, but it is not clear how to compare claims made with different approaches/metrics. Ideally, there would be one

metric which captures all the intuitive properties of unlearning covered by metrics proposed to this day. Our work tackles this problem by first showing that *verification error*—the ℓ_2 difference in weights between an approximately unlearned model and a naively retrained model—implies a large class of the other metrics. Thus it carries a stronger intuition for unlearning, and helps unify the pursuits of other work.

Nevertheless, verification error has its own faults. To measure it, one needs to compute the naively retrained model, which begs the question of why not just use the retrained model as the unlearned model? Furthermore training a model is noisy due to numerical instabilities introduced by back-end randomness in floating point computations, so comparison with respect to any one retrained model leaves the metric itself noisy. It is also not immediately apparent what one should do then to reduce the verification error. Additionally, for verification error to subsume other metrics, the unlearning method should satisfy specific properties (refer § 4.2).

Our work answers these questions. First by breaking down the canonical stochastic gradient descent (SGD) training algorithm with a Taylor series and then further analyzing it, we formalize an unlearning method—*single gradient unlearning*—that only depends on the initial weights (and obtain some other terms that capture approximation error). Thus, unlearning is *approximate* (due to the error term) but *inexpensive* as it depends on only the initial weights.

Second, the analysis leads to an approximation of an unlearned model’s verification error which we call the *unlearning error*. The main advantage of this approximation compared to verification error is that it does not require computing the retrained model (*i.e.*, the ground truth that one would obtain by retraining from scratch to unlearn a point). This makes unlearning error cheaper to compute, and also alleviates the issue of the retrained model being noisy in the computation of verification error. We empirically show that unlearning error is strongly correlated with verification error in relevant contexts. This allows us to envision directly minimizing unlearning error during training, so as to improve our ability to later unlearn with smaller verification error. This is particularly appealing given that unlearning error is expressed in a form where the variables we need to change during training to decrease unlearning error are apparent.

These properties of unlearning error help us (and future efforts building on our work) design approximate unlearning mechanisms with lower verification error. Specifically, we propose our *Standard Deviation (SD) loss* which we show effectively decreases this unlearning error (and verification error); intuitively the standard deviation loss forces the model to converge with less overall change to the weights. This then allows us to unlearn a point from models trained with the SD loss using single gradient unlearning while obtaining a lower unlearning error (and consequently verification error).

To summarize, the main contributions of our work are:

1. A taxonomy of approximate unlearning which concludes

with verification error as a metric to study, given that it implies a large class of unlearning criteria. We characterize how this is not the case for several other metrics proposed.

2. An analysis of SGD which (a) introduces an inexpensive mechanism for unlearning termed single gradient unlearning, and (b) uncovers the variables impacting verification error. This not only yields an easier-to-compute proxy for verification error, but also informs how to train models that are easier to unlearn well.
3. A way of decreasing this unlearning error (and thus in turn verification error) by the use of our SD loss with little impact to performance. We validate our approach empirically on CIFAR-10, CIFAR-100, and IMDB sentiment classification.

2 Primer on Deep Learning & Notation

In our work, we focus on supervised learning [14]. We utilize a bold-faced font to denote vectors (and tensors). We consider a dataset D which consists of pairs $\{(\mathbf{x}_i, y_i)_{i \in [n]}\}$ (where $[n] = \{0, 1, \dots, n-1\}$; \mathbf{x} is a datapoint (*e.g.*, an image) and y is its label. We wish to train a model M , which is a parameterized function of weights \mathbf{w} that we can modify (or learn); mathematically, the model is denoted as the function $M : \mathcal{X} \rightarrow \mathcal{Y}$, where \mathcal{X} denotes the space of inputs (*i.e.*, $\mathbf{x} \in \mathcal{X}$) and \mathcal{Y} denotes the space of outputs (*i.e.*, $y \in \mathcal{Y}$). Ideally, the model should be denoted $M_{\mathbf{w}}$, but we omit the dependence on \mathbf{w} when the context is clear. Our experiments consider deep neural networks (DNNs) given their success on various difficult tasks [15] and the large training costs associated with them.

To learn the weights that make M best classify D , we minimize a loss function \mathcal{L} that measures the error our model has when predicting the label y from an input \mathbf{x} . Examples of such loss functions include the cross-entropy (CE) loss [16] which is the de-facto choice for classification tasks. The cross-entropy loss is defined as:

$$\mathcal{L}_{CE}(M(\mathbf{x}), \mathbf{y}) = - \sum_{i=1}^c y_i \log(M(\mathbf{x})_i) \quad (1)$$

where $M(\mathbf{x})$ returns a probability simplex, and $M(\mathbf{x})_i$ is the i^{th} value in this simplex, and $\mathbf{y} = (y_1, \dots, y_c)$, $y_i \in \{0, 1\}$ is the one-hot vector defining the label of \mathbf{x} , and c is the number of classes. Since a closed form solution cannot be found analytically for non-convex models such as DNNs, the weights \mathbf{w} are learnt in an iterative manner. Many established optimization schemes are derived from mini-batch stochastic gradient descent (SGD) [17]. Formally speaking, mini-batch SGD can be described as below:

$$\mathbf{w}_{t+1} = \mathbf{w}_t - \eta \frac{\partial \mathcal{L}}{\partial \mathbf{w}} \Big|_{\mathbf{w}_t, \tilde{\mathbf{x}}_t}$$

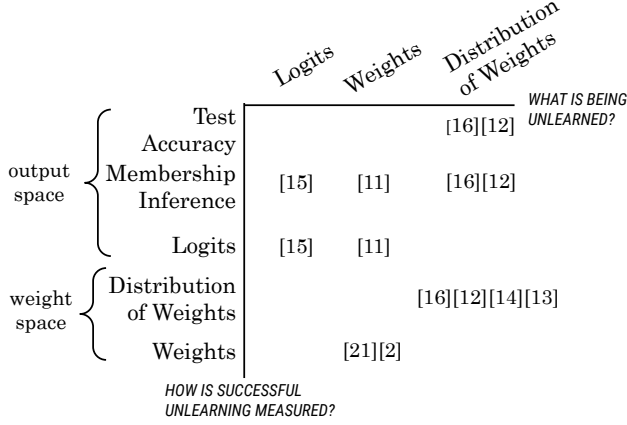


Figure 1: Taxonomy of prior work on post-hoc (post-training) approximate (avoiding retraining) unlearning methods. Unlearning methods are categorized in two ways: (1) What is the definition of unlearning used to motivate the removal of information (horizontal axis)? (2) How is the success of the unlearning method measured (vertical axis)?

where weights at step t are obtained using the weights from step $t - 1$, $\hat{\mathbf{x}}_t$ is the mini-batch of data used at step t , and η denotes the learning rate hyperparameter.

3 Taxonomy of Approximate Unlearning

We begin by discussing the semantics behind unlearning: the problem of *forgetting* a datapoint $\mathbf{x}^* \in D$ from a model M which was trained on it (§ 3.1). We proceed to discuss metrics to measure the efficacy of unlearning (§ 3.2), and methods to achieve them (§ 3.3). Broadly speaking we follow the taxonomy given in Figure 1, with emphasis on specific examples of the metrics (y-axis) and methods (x-axis).

3.1 Defining Unlearning

Let \mathcal{H}_D define the distribution of all models a training rule could return when trained on a dataset D . \mathcal{H}_D is a distribution and not a single point as SGD has inherent stochasticity and there is randomness with back-end floating point operations. Similarly let $\mathcal{H}_{D'}$ represent the distribution of all the models the same training rule returns when trained on dataset $D' = D \setminus \mathbf{x}^*$ where $\mathbf{x}^* \in D$ is the datapoint that is to be unlearned. Lastly, let $U(M, \mathbf{x}^*)$ be some process (randomized or deterministic) that takes a model $M \sim \mathcal{H}_D$ and a data point \mathbf{x}^* , and returns another model M'' . Now if $S = U(\mathcal{H}_D, \mathbf{x}^*)$ is the distribution of \mathcal{H}_D after the transformation by U , we say the process U is an *exact unlearning process* iff $S = \mathcal{H}_{D'}$, i.e., the distribution of output models from $U(\mathcal{H}_D, \mathbf{x}^*)$ is the same distribution as $\mathcal{H}_{D'}$. In this case, $M'' \sim U(M, \mathbf{x}^*)$ is called an unlearned model.

Though this definition looks precise, there is ambiguity with what metric space these models belong to (and consequently for the distributions). A model can be viewed either as just a mapping of inputs to outputs $(\mathbf{x}, M(\mathbf{x}))$ in which case $\mathcal{H}_D, S, \mathcal{H}_{D'}$ are distributions over a function space (i.e., continuous function with the supremum metric), or as the specific parameters \mathbf{w} for an architecture, in which case $\mathcal{H}_D, S, \mathcal{H}_{D'}$ are distributions over the weight space (i.e., some finite dimensional real vector space with the euclidean norm). The ambiguity leads to two notions of *exact unlearning*.

Def 1 $d_w(S, \mathcal{H}_{D'}) = 0$ where d_w measures difference in the *distribution of weights*

Def 2 $d_{out}(S, \mathcal{H}_{D'}) = 0$ where d_{out} measures difference in the *distribution of input-output maps*, or simply difference in the *distribution of outputs*

Naively retraining without \mathbf{x}^* as the unlearning process U guarantees both of these definitions (as we exactly obtain $\mathcal{H}_{D'}$), and is the undisputed baseline for exact unlearning. However the issue with naive retraining is the large computational overhead associated with it (i.e., cost to train a model), especially for large models [18].

Approximate unlearning methods try to alleviate these cost-related concerns. Instead of retraining, these methods execute computationally less expensive operations on the final weights, apply some architectural change, or filter outputs. Approximate unlearning also relaxes the definition of **Def 1** or **Def 2** to requiring the distance between $\mathcal{H}_{D'}$ and S to be small rather than being exactly zero.

Observe that there can be many different metrics d over both of these spaces. Because comparing distributions is expensive (especially if it involves running the training algorithm multiple times to obtain multiple samples), approximate unlearning methods often move away from requiring a measure of the distance d between distributions to instead a measure of an alternative quantity that captures the difference in the weight space or output space on a point basis. For example, a popular approach is to use membership inference to gauge how close two models (before and after unlearning) are in the output space. The popular classes of metrics used are listed on the y-axis of our taxonomy in Figure 1, and what aspect of the model the approximate unlearning methods change to unlearn a datapoint are listed on the x-axis.

3.2 Unlearning Metrics

We now provide some examples of the various unlearning metrics used in past work. This follows the main categories found on the y-axis of Figure 1. Note the first three are metrics over the weight space (i.e., the metrics take as inputs weights or distributions of weights), and the fourth is in the output space (i.e., metrics take as inputs the outputs of the model).

1. ℓ_2 Distance: Here, we compute the weights of a naively retrained model M' and compare them to the weights of the

model M'' that we obtained after using an approximate unlearning process. If they are close, then this suggests that M'' is close to an exactly unlearned model, and can approximate the unlearned model. The standard approach to measure distance in the weight space is the ℓ_2 distance; we term this *verification error* throughout the paper. Such an approach is used by Wu *et al.* [19].

Despite this metric being simple, there are certain drawbacks. First, to compute the verification error, one first needs to compute M' (through naive retraining), which is computationally expensive. If one could obtain M' , then they could avoid approximate unlearning altogether and use that as the unlearned model. Another issue is that one can retrain on the same sequence of data from the same initialization and obtain different terminal weights [20] (which is caused by randomness and numerical instabilities in floating point operations).

2. KL Divergence: To bypass this issue of hardware randomness in training, Golatkar *et al.* [9] consider measuring the similarity of the weights of M'' with respect to a distribution of weights of M' . They achieve this by looking at *Kullback-Leiber (KL) divergence* of the two distributions (as they consider M'' as being the result of another stochastic process on the original model M). The drawback to this are that explicitly calculating the KL divergence requires knowing the final distributions of models trained on D' . This in turn involves sampling many final models trained on D' in order to fit some distribution to the known distribution of M' .

3. Privacy Leakage of Weight Distributions: Another common metric for measuring unlearning that also looks at the distribution of weights is the *privacy leakage from the distribution of weights of M''* (e.g., [21]): ideally, the distribution of weights of M' leaks no information about \mathbf{x}^* as it was not trained on it (though this is not necessarily the case [22]), and so the smaller the privacy leakage of \mathbf{x}^* from the distribution of weights of M'' , the closer M'' is to being unlearned. Sekhari *et al.* [10] analogously present privacy leakage for unlearning in the framework of differential privacy: they bound the leakage of information about a particular \mathbf{x}^* (or more generally a set of datapoints to unlearn) with privacy parameters ϵ, δ and define this as (ϵ, δ) -unlearning. Guo *et al.* [11] work with a similar setup to Sekhari *et al.* [10], though not identical as they consider only the ϵ bound part. In both cases, having (or decreasing) a bound on privacy leakage is presented as unlearning better.

4. Membership Inference: A privacy attack like membership inference (MI) only requires access to the model’s predictions (outputs) to determine whether the unlearned model M'' was or was not trained on the point to be unlearned \mathbf{x}^* . This approach is used by Graves *et al.* [8] and Baumhauer *et al.* [12]. The reasoning here is that as M' was properly retrained without \mathbf{x}^* , a MI attack should return that it was not trained with \mathbf{x}^* ; if a MI attack on M'' also consistently outputs that M'' was not trained with \mathbf{x}^* , then one could argue that their out-

puts are similar. However, such approaches are not *precise*: it is possible a MI attack will give a false positive that M' had indeed trained on \mathbf{x}^* , in which case simply lowering the MI likelihood of \mathbf{x}^* for M'' does not necessarily imply it has unlearned. We revisit the limitations of MI in § 4.1.

3.3 Unlearning Methods

We turn our attention to the following question: *how exactly does one unlearn?* Current approaches are broadly categorized on the x-axis of Figure 1.

Logits: Baumhauer *et al.* [12] consider a specific type of model taking the form $M(\mathbf{x}) = \mathbf{w}f(\mathbf{x})$, where f is some black-box feature extractor, and \mathbf{w} is some parameterized matrix which is what is modified by training. They then unlearn a class from the linear layer *only*. This unlearning is done by defining a filtration matrix and appending it to the model which shifts the outputs to what one would get if one did not train with that class.

Weights: Graves *et al.* [8] proposed amnesiac machine learning, which is an unlearning protocol that logs all the training updates. Then, upon receiving an unlearning request for \mathbf{x}^* , one proceeds to add back all the training updates that involved \mathbf{x}^* to the final weights to obtain an unlearned model M'' .

Distribution of Weights: The scrubbing procedure introduced by Golatkar *et al.* [9, 13] is derived by adding a weighted term to the loss (to measure the KL divergence of the distribution of final weights), and minimizing the added term. Alternatively, differential privacy provides bounds on how indistinguishable a given model is to one not trained on any one of its training datapoints, in essence stating that a model has already unlearned. However Sekhari *et al.* [10] show that differentially private learning only allows one to delete $O(\frac{n}{\sqrt{d}})$ data points while retaining meaningful bounds, and propose an unlearning algorithm for (strongly) convex loss functions that improves the number of datapoints one can delete by adding a Hessian update and noise to the final weights.

4 Verification Error Captures All Metrics

One of the main takeaways from the taxonomy laid out in § 3 is that there are many different metrics for measuring unlearning. Understanding the relationship between these metrics is paramount to concretely understanding the unlearning guarantees they provide. To this end, we focus on unifying the various metrics proposed earlier.

4.1 Weight Metrics encompass Output Metrics

It is intuitive that having similar weights would mean having similar outputs, as clearly if the weights of two models are

identical then so are their outputs. We can formalize this by looking specifically at the verification error defined as $v = \|\mathbf{w}'' - \mathbf{w}'\|_2$ where \mathbf{w}'' are the weights of M'' (the unlearned model) and \mathbf{w}' are the weights of M' (the model unlearned by retraining). With v defined as above, we have for any $\mathbf{x} \in D$ that $\lim_{v \rightarrow 0} \|M'(\mathbf{x}) - M''(\mathbf{x})\|_2 = 0$ under continuity of the outputs of the models as functions of the weights. Here by continuity we mean that fixing the input \mathbf{x} to a model we then have that $M(\mathbf{x})$ is a continuous function of the weights. Thus, $\lim_{v \rightarrow 0}$ entails point-wise convergence of the outputs of M'' to the outputs of M' . Furthermore, note that smooth functions are locally lipschitz. Because DNNs are smooth functions, this relation in the limit sense is thus equivalent to a linear convergence on an upper bound on the ℓ_2 difference between the two models' outputs. This means changes to the differences in weights lead to proportional changes to an upper bound on the ℓ_2 difference in the models' outputs for a datapoint. Thus, we observe that the weight space category of metrics (**Def 1**), and specifically the verification error, imply the output space category of metrics (**Def 2**).

However the opposite does not hold. To see why, consider the following counterexample. If one permutes the weights of a neural network, the model's outputs remain identical [23]. Yet, the verification error would not be 0 after such a permutation, and so having all the outputs be the same does not entail having the same weights.

We further illustrate how output space metrics are unable to capture weight space metrics by considering a MI-based metric from § 3 for the output space metric and verification error for the weight space metric. We empirically show how the privacy risk score (PRS) [24] does not imply verification error (in the sense a decrease in PRS does not imply a decrease in verification error). Specifically, we test the correlation between PRS and verification error after applying an approximate method to unlearn a datapoint \mathbf{x}^* . Here, we choose amnesiac machine learning [8] because it was introduced as an approximate approach to unlearning with a MI-based criterion.¹ To this end, we train the original model M , the naively retrained model M' , and model M'' unlearned using amnesiac unlearning on the CIFAR-10 [26] and CIFAR-100 datasets [26], using the ResNet-18 and VGG-19 architectures [27, 28]. We obtain 27 triplets of M, M'', M' by changing the training settings (*i.e.*, different amounts of training, batch sizes, learning rates *etc.*). For each triplet, we measured the PRS of the unlearned point \mathbf{x}^* on M'' , and the verification error $\|\mathbf{w}'' - \mathbf{w}'\|_2$ (obtained from M'' and M' respectively). The results are presented in Figure 2. Observe that there is little to *no correlation* between PRS (an output space metric) and the verification error (a weight space metric). This illustrates how MI, and in general output space metrics, do not capture weight space definitions (**Def 1**).

¹We reproduced the approach because it was originally evaluated on a MI attack by Yeom *et al.* [25].

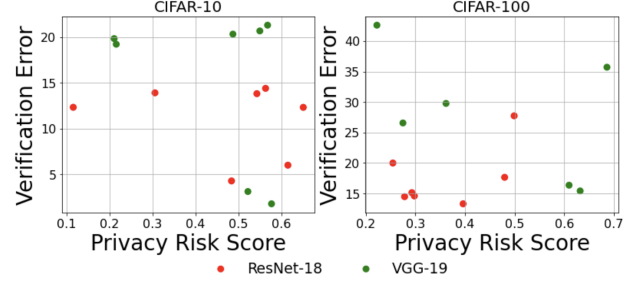


Figure 2: Correlation between privacy risk score and verification error in different training setups for CIFAR-10 and CIFAR-100. The correlations are -0.29 and -0.02, respectively.

4.2 Verification Error implies L^p Weight Metrics

We will prove that verification error provides a bound on the supremum norm of the difference of the distribution of weights obtained by (1) naively retraining, and by (2) using an approximate unlearning method (which depends on the initial weights and batch ordering). Note that a bound on the supremum norm implies bounds on all L^p norms on bounded domains in the weight space. Informally, this allows us to motivate that verification error is an unlearning metric which not only supersedes all output space metrics, but also bounds most weight space metrics. Later in the paper, we will thus consider verification error as the primary metric of interest for unlearning.

Recall the L^p norm of a (lebesgue) measurable function f over a space X is $(\int_X |f|^p d\mu)^{1/p}$ where $d\mu$ is the lebesgue measure [29]. Furthermore, note that by the dominated convergence theorem [29] that all probability density functions can be approximated by a function which has bounded support for arbitrary L^1 error (see Appendix .1). Hence the claim that the bound on the supremum norm implies bounds on *all* L^p metrics.

Similarly, a bound on the supremum norm also implies guarantees similar to differential privacy (DP) (in particular $\epsilon = 0$ and $\delta = b$ where b is the bound on the supremum norm) by the reverse triangle inequality. The opposite, though, is not true when $\epsilon \neq 0$ (as the bound now depends on the magnitude of the function and thus is not uniform). However, it should be noted that in our subsequent analysis, we make several assumptions about the stochasticity of training which does not allow us to derive strict DP-like guarantees. In particular we will assume: (1) noise is simply added to the final weights (to approximate step-wise noisiness), and (2) that this noise changes negligibly when removing a data point from the dataset. We explain why we made these assumptions later in the section during our derivation.

In particular, the focus here will be first comparing the

probability distributions of final weights obtained by training m epochs starting at a fixed initial weight \mathbf{w}_0 with dataset D and dataset $D' = D \setminus \mathbf{x}^*$ with SGD (and not mini-batch SGD, *i.e.*, considering mini-batch sizes of 1). We will represent the density functions respectively as $\mathbb{P}(\mathbf{w})$ and $\mathbb{P}'(\mathbf{w})$ where both are functions of the weights of the model \mathbf{w} , and note in what follows \mathbf{x}^* is fixed but can be any data point (*i.e.*, is a constant).

Let the size of D be $|D| = n$, and let $I = \{\mathbf{x}_{i_1}, \mathbf{x}_{i_2}, \dots, \mathbf{x}_{i_m}\}$ denote a particular ordering of the datapoints when training on D for m epochs (where $i_j \in [n]$). Note that we have $(n!)^m$ such combinations; for D' , we have $(n-1)^m$ such combinations. For each I , there exists an I' (corresponding to $D' = D \setminus \mathbf{x}^*$), which is formed by removing all instances of \mathbf{x}^* (in-place) from I . Note that for a given I' , we have n^m corresponding choices of I (as for each epoch we have n choices to place \mathbf{x}^* per epoch, and m epochs in total). Let \mathbf{w}_I represent the deterministic final weights resulting from training with the data ordering I , starting from \mathbf{w}_0 . Let \mathbf{g} denote the random variable which represents the noise on the final weights (*i.e.*, we assume the noise per step accumulates so we can simply add some random variable onto the final weights) when training for $m \cdot n$ steps. Thus, the random variable representing the final weights when training with I is $\mathbf{z}_I = \mathbf{w}_I + \mathbf{g}$. Similarly, we define $\mathbf{z}_{I'} = \mathbf{w}_{I'} + \mathbf{g}'$ where \mathbf{g}' represents the noise when training $(n-1) \cdot m$ steps. Note that, if training is deterministic, we have $\mathbf{w}_{I'} = \mathbf{w}_I - \mathbf{d}_I$ where \mathbf{d}_I is some constant that only depends on \mathbf{w}_0 and the ordering I (as under deterministic operations $\mathbf{w}_{I'}$ and \mathbf{w}_I are constants depending only on \mathbf{w}_0 and the ordering I and thus $\mathbf{w}_I - \mathbf{w}_{I'} = \mathbf{d}_I$ is a constant that only depends on them). Lastly, we make an assumption that the noise from training with $m \cdot n$ steps is equivalent to that training from $(n-1) \cdot m$ steps, *i.e.*, that $\mathbf{g} = \mathbf{g}'$. This is based on the fact that this noise should only be a function of the number of training steps, and that noise per step is small (see [20, § 6] for a discussion on noise during training)². Thus we have $\mathbf{z}_{I'} = \mathbf{z}_I - \mathbf{d}_I$.

Given that SGD samples individual datapoints uniformly, the probability of obtaining a given data ordering is constant. Further, if $\mathbb{P}_I(\mathbf{w})$ is the density function corresponding to \mathbf{z}_I and $\mathbb{P}'_{I'}(\mathbf{w})$ is the density function corresponding to $\mathbf{z}_{I'}$ (which is equal to $\mathbb{P}_I(\mathbf{w} - \mathbf{d}_I)$), then $\mathbb{P}(\mathbf{w}) = \frac{1}{n!^m} \sum_I \mathbb{P}_I$ and $\mathbb{P}'(\mathbf{w}) = \frac{1}{(n-1)!^m} \sum_{I'} \mathbb{P}'_{I'}(\mathbf{w})$.

Lemma 1. *If every \mathbb{P}_I is Lipschitz with Lipschitz constant L (which is true if \mathbf{g} is gaussian), and if we let $d = \frac{1}{n!^m} \sum_I \|\mathbf{d}_I\|_2$, then:*

$$\|\mathbb{P}(\mathbf{w}) - \mathbb{P}'(\mathbf{w})\|_2 \leq L \cdot d \quad (2)$$

We refer the reader to Appendix .1 for the detailed derivation. This result shows that by accounting for all the individual distributions (for each ordering I), we were able to

²Thus, adding or removing m steps (1 per epoch) when compared to the $m \cdot n$ total steps when training with ordering I is insignificant

obtain a Lipschitz condition on the combined distribution (of final weights obtained by training m epochs starting at a fixed initial weight \mathbf{w}_0). The Lipschitz condition is expressed with respect to the datasets including or excluding the point to be unlearned.

Now, we are also interested in the difference between the density function obtained after the application of an approximate unlearning method on M (*i.e.*, $\mathbb{P}''(\mathbf{w})$), and $\mathbb{P}'(\mathbf{w})$. If the approximate unlearning method only considers \mathbf{w}_0, I to define an unlearning update \mathbf{u}_I , and obtains the approximately unlearned weights by adding \mathbf{u}_I to \mathbf{w}_I , *i.e.*, $\mathbf{w}''_I = \mathbf{w}_I + \mathbf{u}_I$, then:

Corollary 1. *If every \mathbb{P}_I is Lipschitz with constant L (true if \mathbf{g} is gaussian), and if we let $v = \frac{1}{n!^m} \sum_I \|\mathbf{d}_I + \mathbf{u}_I\|_2$, then:*

$$\|\mathbb{P}''(\mathbf{w}) - \mathbb{P}'(\mathbf{w})\|_2 \leq L \cdot v \quad (3)$$

The detailed proof is in Appendix .1. This naturally follows from the same accounting procedure used for the previous lemma, but now \mathbf{d}_I have been swapped for $\mathbf{d}_I + \mathbf{u}_I$. This gives us a bound on the supremum norm by the average verification error v (times some constant) on the difference of the probability distributions after approximate unlearning $\mathbb{P}''(\mathbf{w})$ and ideal retraining $\mathbb{P}'(\mathbf{w})$. Note, however, that there is a necessary assumption on the form of this approximate unlearning method: to obtain Equation 3, we require the unlearning update to only be dependant on the initial weight \mathbf{w}_0 and I . We will introduce such an unlearning approach in § 5. Finally, an analogous bound going in the opposite direction is provided in Appendix .1.

Summary: In § 4.1, we demonstrated how verification error captures the changes in outputs, and thus encompasses metrics that measure unlearning using Def 2. We then proceeded to demonstrate how, using a particular form of approximate unlearning (and assumptions about noise), verification error also leads to uniform bounds in the difference in weight distributions of M' (the retrained model) and M'' (the approximately unlearned model). Thus, verification error also encompasses a large class of metrics that measure unlearning using Def 1.

5 Defining the Unlearning Error

Recall that verification error's strongest limitation is the expense associated with calculating it (*i.e.*, the requirement for naive retraining). To circumvent this issue, we set out to approximate verification error. Our analysis seeks to understand the deterministic impact of a data point \mathbf{x}^* on the final weights of a model when trained with SGD starting at initial weights \mathbf{w}_0 . We expand the recursive updates performed by SGD to isolate terms that can be easily unlearned (because they do not depend on the order of data points) from terms that are difficult to unlearn. We then obtain and analyze a closed form

approximation of these terms. This results in (a) a proxy metric (which we term *unlearning error*) that captures the effects of the verification error, and (b) an inexpensive approximate unlearning method that only depends on \mathbf{w}_0 and so allows us to use the bounds presented in § 4.

5.1 Expanding SGD

To understand the impact of a data point \mathbf{x}^* on the final weights, we need to expand a sequence of SGD updates. We begin with the definition of a single SGD learning update:

$$\mathbf{w}_1 = \mathbf{w}_0 - \eta \frac{\partial \mathcal{L}}{\partial \mathbf{w}}|_{\mathbf{w}_0, \hat{\mathbf{x}}_0}$$

where \mathbf{w}_0 denotes the weights at step 0 and $\hat{\mathbf{x}}_0$ denotes the data sampled at step 0. Note, we make no constraints on what \mathbf{w}_0 is (that is where training starts from), *i.e.*, could start from a pre-trained model). We obtain \mathbf{w}_2 , the weight obtained at step 2, as follows:

$$\begin{aligned} \mathbf{w}_2 &= \mathbf{w}_0 - \eta \frac{\partial \mathcal{L}}{\partial \mathbf{w}}|_{\mathbf{w}_0, \hat{\mathbf{x}}_0} - \eta \frac{\partial \mathcal{L}}{\partial \mathbf{w}}|_{\mathbf{w}_1, \hat{\mathbf{x}}_1} \\ \implies \mathbf{w}_2 &= \mathbf{w}_0 - \eta \frac{\partial \mathcal{L}}{\partial \mathbf{w}}|_{\mathbf{w}_0, \hat{\mathbf{x}}_0} - \eta \frac{\partial \mathcal{L}}{\partial \mathbf{w}}|_{\mathbf{w}_0 - \eta \frac{\partial \mathcal{L}}{\partial \mathbf{w}}|_{\mathbf{w}_0, \hat{\mathbf{x}}_0}, \hat{\mathbf{x}}_1} \end{aligned}$$

This can further be expanded and approximated as follows:

$$\mathbf{w}_2 \approx \mathbf{w}_0 - \eta \left(\frac{\partial \mathcal{L}}{\partial \mathbf{w}}|_{\mathbf{w}_0, \hat{\mathbf{x}}_0} + \frac{\partial \mathcal{L}}{\partial \mathbf{w}}|_{\mathbf{w}_0, \hat{\mathbf{x}}_1} + \frac{\partial^2 \mathcal{L}}{\partial^2 \mathbf{w}}|_{\mathbf{w}_0, \hat{\mathbf{x}}_1} \left(-\eta \frac{\partial \mathcal{L}}{\partial \mathbf{w}}|_{\mathbf{w}_0, \hat{\mathbf{x}}_0} \right) \right)$$

Our end goal is informed by our analysis in § 4: we *must* focus on an analysis of verification error in SGD that is only a function of the initial weights \mathbf{w}_0 and the ordering of es of data I . To scale the above for a sequence of t updates, notice that the Hessian terms from the expansion recursively depend on each other. Thus we have the final approximation:

$$\mathbf{w}_t \approx \mathbf{w}_0 - \eta \sum_{i=0}^{t-1} \frac{\partial \mathcal{L}}{\partial \mathbf{w}}|_{\mathbf{w}_0, \hat{\mathbf{x}}_i} + \sum_{i=1}^{t-1} f(i) \quad (4)$$

where $f(i)$ is defined recursively as:

$$f(i) = -\eta \frac{\partial^2 \mathcal{L}}{\partial^2 \mathbf{w}}|_{\mathbf{w}_0, \hat{\mathbf{x}}_i} \left(-\eta \sum_{j=0}^{i-1} \frac{\partial \mathcal{L}}{\partial \mathbf{w}}|_{\mathbf{w}_0, \hat{\mathbf{x}}_j} + \sum_{j=0}^{i-1} f(j) \right) \quad (5)$$

with $f(0) = 0$.

Understanding the Approximation From Equation 4, observe that one can represent the weights obtained after training t updates as the sum of two sums. We now wish to understand how \mathbf{x}^* affects this expression (and thus the approximate outcome of training). The terms in the *first sum* are simply gradients taken with respect to the initial weights \mathbf{w}_0 and $\hat{\mathbf{x}}_i$ following the order we give data to the model. Notice, however, that the exact order does not matter as we are simply

adding them. In this case, it is clear that the effect of \mathbf{x}^* (provided at any step in training) on this first sum is a gradient (or gradients) computed with respect to \mathbf{w}_0 and \mathbf{x}^* .

Single gradient unlearning: To reverse this effect and unlearn, we simply have to *add back these gradients* which amounts to adding $\frac{\eta m}{b} \frac{\partial \mathcal{L}}{\partial \mathbf{w}}|_{\mathbf{w}_0, \mathbf{x}^*}$ to the final weights, where η is the learning rate, b is the batch size, and m is the number of epochs (which is the number of copies of this gradient that are present in the first sum).

The *second sum* is more complex as the expression is recursive, and so there is an inherent dependence on order. Understanding this sum will be our focus in § 5.2. One of the main takeaways is that to compute all the terms that contain a particular \mathbf{x}^* , one would have to spend at least as much compute as training. For this reason, *the process to unlearn the first sum will be our unlearning method*, and our analysis of the second sum (which we do not unlearn) will result in an *inexpensive proxy metric* for the verification error which makes clear key variables one should focus on to decrease verification error.

5.2 Approximating the Second Sum Series

The global structure of the second sum follows $\eta^2 \mathbf{c}_t + \eta^3 \mathbf{c}_{t-1} + \dots + \eta^{2+t-1} \mathbf{c}_1$, where \mathbf{c}_i represents some vector. Thus, we can focus primarily on the η^2 dependent term as, in practice, we often observe η being a magnitude or more less than 1, and so η^2 is the dominant term. Thus, the second sum can be approximated as:

$$\eta^2 \mathbf{c}_t = \sum_{i=1}^{t-1} \eta^2 \frac{\partial^2 \mathcal{L}}{\partial^2 \mathbf{w}}|_{\mathbf{w}_0, \hat{\mathbf{x}}_i} \sum_{j=0}^{i-1} \frac{\partial \mathcal{L}}{\partial \mathbf{w}}|_{\mathbf{w}_0, \hat{\mathbf{x}}_j} \quad (6)$$

We can further approximate $\sum_{j=0}^{i-1} \frac{\partial \mathcal{L}}{\partial \mathbf{w}}|_{\mathbf{w}_0, \hat{\mathbf{x}}_j}$ by its expectation $\frac{i(\mathbf{w}_t - \mathbf{w}_0)}{t}$. We further normalize the vector, and thus have:

$$\eta^2 \mathbf{c}_t \approx \eta^2 \frac{\|\mathbf{w}_t - \mathbf{w}_0\|_2}{t} \sum_{i=1}^{t-1} \frac{\partial^2 \mathcal{L}}{\partial^2 \mathbf{w}}|_{\mathbf{w}_0, \hat{\mathbf{x}}_i} \frac{\mathbf{w}_t - \mathbf{w}_0}{\|\mathbf{w}_t - \mathbf{w}_0\|_2} i \quad (7)$$

By focusing on $\|\mathbf{c}_t\|_2$, note that

$$\left\| \frac{\partial^2 \mathcal{L}}{\partial^2 \mathbf{w}}|_{\mathbf{w}_0, \hat{\mathbf{x}}_i} \frac{\mathbf{w}_t - \mathbf{w}_0}{\|\mathbf{w}_t - \mathbf{w}_0\|_2} \right\|_2 \leq \left\| \frac{\partial^2 \mathcal{L}}{\partial^2 \mathbf{w}}|_{\mathbf{w}_0, \hat{\mathbf{x}}_i} \right\|_2$$

by definition of the induced ℓ_2 norm, which is simply the square root of the largest eigenvalue of the Hessian *i.e.*, $\sigma_{1,i}$ the first singular value of the Hessian on $\hat{\mathbf{x}}_i$. For sake of simplicity we consider $\sigma = \max(\sigma_{1,i})$, and thus have the following inequality:

$$\|\eta^2 \mathbf{c}_t\|_2 \leq \eta^2 \frac{\|\mathbf{w}_t - \mathbf{w}_0\|_2}{t} \cdot \sigma \cdot \frac{t(t-1)}{2} \quad (8)$$

Thus, we can observe that the second sum linearly depends on $\|\mathbf{w}_t - \mathbf{w}_0\|_2$, σ , and t . σ captures the non-linearity of the loss landscape from the Hessian, and thus we see that the more linear the loss landscape, the tighter this bound on the approximation. We also see from this that in the scenario $t = 1$ or $\sigma = 0$, this bound, and thus the term, is 0 reinforcing the notion that if the loss landscape was just linear we could get away with just focusing on the first sum of gradients.

Counting Terms: Now, with an understanding of what the dominant terms in the second sum of Equation 4 are, we take a step back and ask whether it is possible to unlearn \mathbf{x}^* from these. What we will do is count all the terms involving \mathbf{x}^* and show that to compute those in order to remove their affect is computationally expensive (and thus we can not reasonably improve our single-gradient unlearning method). Specifically, we focus on the expression in Equation 6. We let i^* denote the first index where \mathbf{x}^* appears, and we are interested in those terms that contain $\hat{\mathbf{x}}_{i^*}$ (and thus \mathbf{x}^*). These are the terms that we would need to remove in order to forget $\hat{\mathbf{x}}_{i^*}$ from the dominant terms in our second sum in Equation 4. Note then that this will actually be an undercount, as \mathbf{x}^* could appear in another batch, so the final cost we state will be less than what we actually need to completely forget \mathbf{x}^* .

The first thing to note is that $\hat{\mathbf{x}}_{i^*}$ does not appear in any terms in the expression until $i = i^*$. For this index, we have i^* terms dependent on $\hat{\mathbf{x}}_{i^*}$ as every term in the second sum in Equation 6 is multiplied by $\frac{\partial^2 \mathcal{L}}{\partial^2 \mathbf{w}}|_{\mathbf{w}_0, \hat{\mathbf{x}}_{i^*}}$. Now for all the indices $i > i^*$ (i.e., $t - 1 - i^*$ indices), we have exactly one term with $\hat{\mathbf{x}}_{i^*}$ which comes from a $\frac{\partial^2 \mathcal{L}}{\partial^2 \mathbf{w}}|_{\mathbf{w}_0, \hat{\mathbf{x}}_{i^*}}$ appearing in the second sum. In total, we have $(t - 1 - i^*) + i^* = t - 1$ terms, and note that all these terms are Hessian vector products (because all the terms in Equation 6 are Hessian vector products). In general, it is possible to implement Hessian products in $O(n)$ [30].

Importantly, these Hessian vector products are at least as expensive as a gradient computation. In the case batch size $b = 1$, this would be equivalent to the cost for training, and in general is $\frac{1}{b}$ the cost of training as we only need to compute 1 of the b gradients in the batch, i.e., just with respect to \mathbf{x}^* . However this can still be a significant amount in practice (as t here is not the number of epochs but the number of individual training steps), and so from counting the terms with \mathbf{x}^* we see that this second sum in Equation 4 (which we can approximate with Equation 6) is a bound to how well we can reasonably forget the effect of \mathbf{x}^* .

5.3 Unlearning Error

Based on the above discussion for estimating the second sum, and how it bounds how well we can unlearn (without adding on significant computational costs), we define Equation 8 to be our *unlearning error* (e). In practice, we make a slight modification as this bound can be loose; we take σ to be the average of all the $\sigma_{1,i}$ rather than the max, as to better approximate Equation 6. To be precise, defining $\sigma_{avg} = \frac{1}{t} \sum_{i=1}^t \sigma_{1,i}$,

we define unlearning error as:

$$e = \eta^2 \cdot \frac{\|\mathbf{w}_t - \mathbf{w}_0\|_2}{t} \cdot \sigma_{avg} \cdot \frac{t^2 - t}{2} \quad (9)$$

Working with the average also allows one to only compute $\sigma_{1,i}$ every couple of steps, saving costs. Lastly, computing e does not require us to have applied our unlearning method first; we can preemptively know what the unlearning error e will be.

6 Reducing the Unlearning Error

In § 5, we identified terms of SGD which force (post-training) approximate unlearning approaches to incur verification error. Our unlearning error captures these effects through the number of steps t , the average singular value σ_{avg} , and the difference between final and initial weights $\|\mathbf{w}_t - \mathbf{w}_0\|_2$. Our closed form approximation of SGD from the previous section leads to an unlearning method (see gray box in § 5) that only depends on the initial weights \mathbf{w}_0 . We now introduce modifications to the training procedure, which are orthogonal to the unlearning method itself but reduce the values of the different variables contributing to unlearning error. This therefore yields a training algorithm which makes it easier to later unlearn with our method at a minimal verification error.

6.1 Strawman Approaches

We first consider two³ strawman approaches, each trying to directly minimize one of three factors identified in the unlearning error formulation: the number of steps t and the difference between final and initial weights $\|\mathbf{w}_t - \mathbf{w}_0\|_2$.

1. Training for Less: From Equation 9, recall that unlearning error e depends on number of steps t . A simple method to reduce e would be to train for fewer steps. We verify empirically if training for less steps t reduces e .

Our evaluation is performed on two canonical architectures for computer vision, ResNet-18 [27] and VGG-19 [28], on two vision datasets, CIFAR-10 [26] and CIFAR-100 [26]. The datasets consist of 60000 $32 \times 32 \times 3$ images that belong to 10 and 100 classes respectively. The classes include animals and objects. This leads to four settings (one for each model and dataset combination). For a dataset D , we denote by M_t the model trained on D for t training steps starting from M_0 ; in the experiments we compute the unlearning error from M_0 to M_t , and record the intermediate values of e .

³We also tried several other ideas at reducing unlearning error which we do not describe in great detail here. One such idea was trying to reduce σ_{avg} by adding a regularization term with the sum of the diagonal entries of the Hessian of CE loss with respect to the logits squared (which are of the form $\{p_1(1-p_1), \dots, p_c(1-p_c)\}$ where p_i is the softmax output of logit $M(\mathbf{x})_i$, but as will be theme with this section, we saw no benefit.

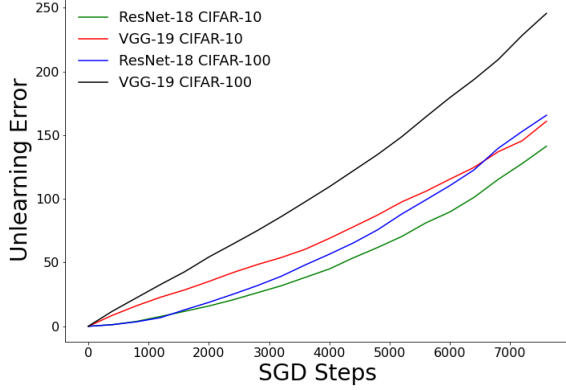


Figure 3: Unlearning error for 4 different settings as a function of the number of finetuning steps. Across all 4 settings, the unlearning error increases as a function of t . Each model was trained for $t = 7812$ steps (5 epochs)

Figure 3 illustrates how e increases (practically linearly) with t . This implies that by training less, we decrease e almost proportionally. This however also degrades the model’s performance (*i.e.*, prediction accuracy) which creates an undesirable trade-off. One way to alleviate this limitation would be to pre-train the model on a public dataset so as to start training at a better initialization and compensate for the lower number of training steps performed on data that may be unlearned. However, it is not always possible to find a public dataset for which no unlearning requests will be issued.

2. ℓ_2 Regularization. The next factor involved in the unlearning error e is the weight difference $\|\mathbf{w}_t - \mathbf{w}_0\|_2$; decreasing this term (while not changing anything else) would also decrease e . By the triangle inequality, we have that $\|\mathbf{w}_t - \mathbf{w}_0\|_2 \leq \|\mathbf{w}_t\|_2 + \|\mathbf{w}_0\|_2$ and so it would seem that by decreasing either $\|\mathbf{w}_t\|_2$ or $\|\mathbf{w}_0\|_2$, we might be able to obtain a tighter bound on $\|\mathbf{w}_t - \mathbf{w}_0\|_2$ and decrease it. This reasoning motivates using ℓ_2 regularization which decreases the norm of the final weights $\|\mathbf{w}_t\|_2$ by adding a $\lambda\|\mathbf{w}\|_2$ regularization term (where λ is a regularization constant) to the CE loss.

To evaluate this regularizer, we use the same setup that was previously described. We repeat the experiments for different values of regularization strength: we pick $\lambda \in \{0.0, 0.001, 0.01, 0.1\}$. In Figure 4, we track e for $t = 7812$ training steps (5 epochs) for the two CIFAR-10 models (Table 3 includes CIFAR-100 results) and the various strengths of ℓ_2 regularization. We observe that there was no consistent benefit to employing the loss penalty, and in most cases it in fact increased e . The main issue is that the bound $\|\mathbf{w}_t - \mathbf{w}_0\|_2 \leq \|\mathbf{w}_t\|_2 + \|\mathbf{w}_0\|_2$ is very loose and we can decrease the right hand side without decreasing the left hand side (the part which we are interested in) as seen in Figure 14. Thus, we next refine our analysis to obtain a tighter bound and a more effective regularization penalty.

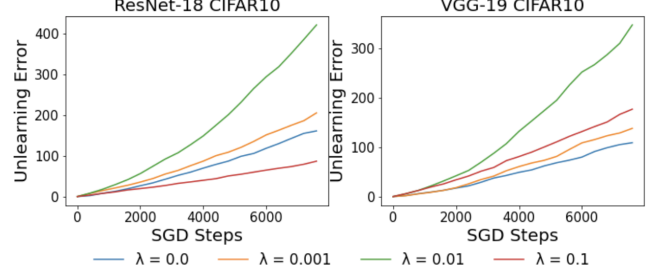


Figure 4: Unlearning error of 4 setups trained with increasing strength of ℓ_2 regularization. As shown, weight decay does not decrease the unlearning error consistently.

6.2 Our Proposal: Standard Deviation Loss

In § 6.1, we considered two strawman approaches: decreasing training steps t and ℓ_2 regularization. What we proceed to do in this section is one of the main contributions of this work: we introduce our own novel standard deviation regularizer. By way of studying a binary linear classifier, we show how it would (when training on an arbitrary, single data point) decrease the final change in weights by moving the minimum of the loss closer to the initial weights. Observe then that as long as this loss does not also increase the singular values (which we later empirically show in § 8.2), it decreases the unlearning error e . Informally, the loss yields a model whose weights required smaller steps to get to during gradient descent from the weights training was initialized with. This explains why unlearning the contributions of a point to these steps using our single gradient approach leads to a smaller unlearning error when the model was trained with our loss. This loss, which we will call standard deviation (SD) loss, is defined as follows:

$$\begin{aligned} \mathcal{L}_{SD}(M(\mathbf{x}), \mathbf{y}) \\ = \mathcal{L}_{CE}(M(\mathbf{x}), \mathbf{y}) + \gamma \sqrt{\left(\sum_{i=1}^c (M(\mathbf{x})_i - \mu)^2\right)/c} \quad (10) \end{aligned}$$

where c is the output dimension of the model M , γ is the regularization strength, and μ is the average value of the output logits $M(\mathbf{x})$ for a specific datapoint \mathbf{x} . Note that the SD loss is simple to integrate into a training framework as it just requires adding a regularization term to the loss function.

A Simple Binary classifier

Next, we illustrate our intuition behind the SD loss with the case of a binary linear classifier (*i.e.*, a linear model with just two outputs) trained to minimize its loss on a single datapoint; we show how the SD loss reduces the minimum distance (in the weight space) to the minimum of the loss (which is where the final weights are found). This results in a

lower weight difference $\|\mathbf{w}_t - \mathbf{w}_0\|_2$, which in turn reduces unlearning error. This holds as long as the SD loss does not also simultaneously increase other variables involved in the definition of our unlearning error, *e.g.*, singular values. We confirm later in § 8.1 that this is the case (even for the neural networks we considered in our evaluation).

Let us consider the specific setup where \mathbf{x} is a vector of length k representing a datapoint, $\mathbf{w} = \begin{bmatrix} \mathbf{w}_1 \\ \mathbf{w}_2 \end{bmatrix}$ is a $2 \times k$ weight matrix, and M is a linear model with two outputs defined by $M(\mathbf{x}) = \mathbf{w}\mathbf{x}$. For the sake of simplicity (and without loss of generality) let us assume the label of \mathbf{x} is 0. Then, the SD loss of our model, where $a = M(\mathbf{x})_1$ and $b = M(\mathbf{x})_2$ (*i.e.*, the first and second output), is:

$$\mathcal{L}_{SD}(M(\mathbf{x}), 0) = -\log\left(\frac{e^a}{e^a + e^b}\right) + \gamma \sqrt{\frac{a^2 + b^2 - 0.5(a+b)^2}{2}} \quad (11)$$

where the second term is just a simplified version of the standard deviation.

The main empirical observation motivating the following analysis is the following: increasing the strength of γ moves the minimum of the SD loss with respect to the outputs a and b (given by Equation 11) closer to the line defined by $a = b$. This is illustrated in Figure 5 where we plot the gradients of our loss with respect to the outputs to observe where they are 0 (*i.e.*, when the direction flips). Similarly, Figure 6 illustrates how the minimum of the loss approaches the line $a = b$ (in black), and generally how the minimum is defined by a line $a = b + \epsilon$ where ϵ decreases with the strength of γ .

We now proceed to analytically show how SD loss reduces the minimum change in weights required to reach a minimum of the loss (for a binary linear classifier). We focus on the initialization of \mathbf{w} by a constant (that is all the entries are the same), and thus $a_0 = \mathbf{w}_1 \cdot \mathbf{x} = \mathbf{w}_2 \cdot \mathbf{x} = b_0$. To find the minimum distance in the weights space to a minimum of the loss, we need to solve the constrained optimization problem

$$\begin{aligned} \min_{\mathbf{u}_1, \mathbf{u}_2} & \|\mathbf{u}_1\|_2^2 + \|\mathbf{u}_2\|_2^2 \\ \text{subject to} & \\ a_0 + \mathbf{u}_1 \cdot \mathbf{x} = b_0 + \mathbf{u}_2 \cdot \mathbf{x} + \epsilon & \\ \implies (\mathbf{u}_1 - \mathbf{u}_2) \cdot \mathbf{x} - \epsilon = 0 & \end{aligned} \quad (12)$$

where \mathbf{u}_1 and \mathbf{u}_2 are the updates to \mathbf{w}_1 and \mathbf{w}_2 respectively to reach the minimum of the loss.

The solution, given by minimizing the lagrangian $\mathcal{L} = \mathbf{u}_1 \cdot \mathbf{u}_1 + \mathbf{u}_2 \cdot \mathbf{u}_2 + \lambda((\mathbf{u}_1 - \mathbf{u}_2) \cdot \mathbf{x} - \epsilon)$, is $\mathbf{u}_1 = \frac{\epsilon}{2\|\mathbf{x}\|_2^2} \mathbf{x}$ and $\mathbf{u}_2 = \frac{-\epsilon}{2\|\mathbf{x}\|_2^2} \mathbf{x}$. Note that $\|\mathbf{u}_1\|_2^2 + \|\mathbf{u}_2\|_2^2 = \frac{\epsilon^2}{2} \|\mathbf{x}\|_2^2$, and by reducing ϵ we reduce the magnitude of the change of weights needed to reach a minimum of the loss. As increasing the strength of our SD loss regularization (γ) does just that, we see that increasing γ means decreasing the minimum change in weights needed to reach a minimum (which is what the path following negative gradients approximates). Thus, if the SD loss does not (also) increase the singular values, it decreases

the unlearning error. As a final remark, we showed that a state with $a = b$ is close to a minimum, but this implies a more general result of just being close to such a state where $a = b$ (*i.e.*, having low standard deviation in the outputs) means being close to the minimum.

7 Implementation

All of the experiments we describe next (and those performed in § 6.1) were conducted on T4 Nvidia GPUs with 16 GB of dedicated memory. We used Intel Xeon Silver 4110 CPUs with 8 cores each and 32GB of RAM. The underlying OS is Ubuntu 18.04.2 LTS 64 bit. We use `pytorch` v1.8.1 with CUDA 10.2 and `python` 3.7. We used the same datasets and models as described in § 6.1. We also evaluate our proposal on a different domain, *text*, using a pre-trained DistilBERT [31] fineuned on IMDB reviews [32] for sentiment analysis (a binary classification task); note IMDB has 25,000 training and test datapoints consisting of sentences of varying lengths which we truncated to the first 512 tokens (the maximum DistilBert takes as input).

8 Evaluation

Through our evaluation, we wish to answer the following questions.

1. Does SD loss decrease unlearning error?
2. How are the various components of the unlearning error (t , σ_{avg} , $\|\mathbf{w}_0 - \mathbf{w}_t\|_2$) affected by training with SD loss?
3. Does decreasing unlearning error (either using SD loss or changing t) result in a decrease in verification error?

To answer the questions above, we utilize our single gradient unlearning approach to obtain the approximately unlearned model. Our salient results are:

1. In § 8.1, we conclude that the proposed SD loss is effective at decreasing the unlearning error. This is achieved at a moderate penalty to accuracy (< 3 percentage points in the setups we tested).
2. In § 8.2, we see that SD loss significantly decreases the final change in weights $\|\mathbf{w}_0 - \mathbf{w}_t\|_2$, and that the impact of SD loss for a given regularization strength is concentrated at the beginning of training
3. In § 8.3, we see that decreasing unlearning error with any of the methods we have considered also decreases verification error (*i.e.*, they are strongly correlated) showing that unlearning error serves as a good proxy metric.

8.1 SD Loss Decreases Unlearning Error

Recall that we introduce the SD loss as a method to reduce the unlearning error as training commences. We wish to

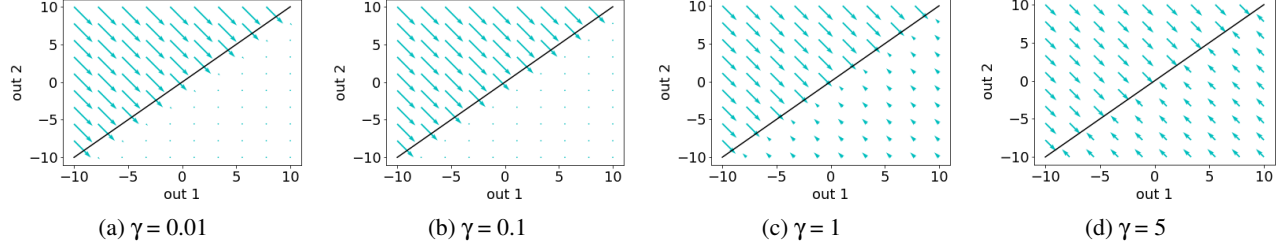


Figure 5: Plots of the negative gradients of SD loss with respect to the two outputs ($a = out1, b = out2$). The black line represents $a = b$. Observe how the minimum of the loss landscape (where the arrows switch direction) approaches the black line.

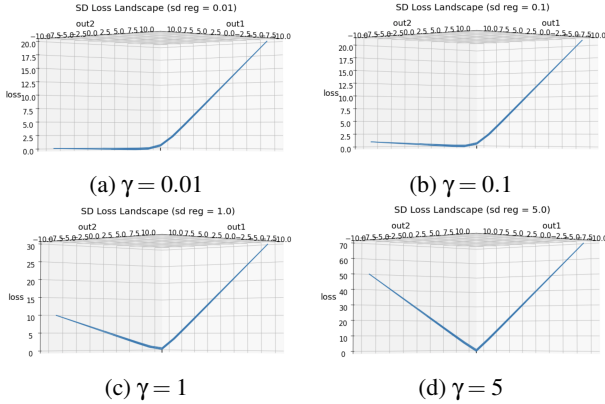


Figure 6: Plots of the SD loss landscape with respect to the two outputs ($a = out1, b = out2$). Note the black dot represents where $a = b$, and observe how the minimum of the loss landscape approaches the black dot

empirically validate this. We utilize the implementation setup details described in § 7, and the following setup:

1. Train M_0 on D with SD loss for N pre-training steps to obtain M_N .
2. Train M_N for an additional t steps on $\hat{\mathbf{x}}_1, \hat{\mathbf{x}}_2, \dots, \hat{\mathbf{x}}_t$ (from D) to get M_{N+t} .
3. Compute the unlearning error (Equation 9) of M_{N+t} starting from M_N , except here \mathbf{w}_t is the weights of M_{N+t} and \mathbf{w}_0 are the weights of M_N .

In this setup, N is a configurable parameter which allows us to understand how the amount of training affects the impact of SD loss on unlearning error (see § 8.2). For the vision models, we utilize $N = 0, 15625, 31250, 46875, 62500, 78125$ steps (*i.e.*, 0, 10, 20, 30, 40, 50 epochs, respectively). For the regularization strength, we use $\gamma = 0, 1, 5, 10, 15, 20$ for CIFAR-10 and $\gamma = 0, 50, 100, 150, 200, 250$ for CIFAR-100 in our experiments. In the case of DistilBERT fine-tuned on IMDB reviews, we observed we reached peak accuracy after just $N = 4688$ steps (or 3 epochs) and simply evaluated that for $\gamma = 0.0, 0.01, 0.05, 0.1, 0.15, 1.0, 1.25, 1.5$ and discuss that in

dependent of t .⁴

Results: In Figure 7, we plot the unlearning error as a function of the number of training steps t . Observe that, as expected, the unlearning error grows as the training duration increases. However, increasing the regularization parameter γ (from 0 *i.e.*, CE loss, to > 0 values) reduces the rate or growth, and thus the final unlearning error. This is consistent with the final unlearning errors we observed for DistilBERT in Table 2 where we see increasing regularization dropped final unlearning error by $40\times$.

The influence of SD loss on the accuracy of the final (vision) models is presented in detail Table 4 in Appendix .3; Table 1 highlights results from our experiments with CIFAR-10 for $N = 10$ epochs. Results for DistilBERT experiments are in Table 2. For the vision models, note that as we increase the value of γ , the accuracy of the classifier learnt decreases. From Table 1), the decrease is within 5 percentage points for values of $\gamma \leq 5$. For values of $\gamma > 5$, the drop in accuracy is larger. This can be explained by having to fit to the dataset while also balancing the requirement of minimizing $\|\mathbf{w}_t - \mathbf{w}_0\|_2$. We will demonstrate this effect in more detail in § 8.2. However, observe that the experiments with DistilBERT indicate a subtle increase in accuracy even after the regularization had cut the unlearning error by $2.5\times$, suggesting some domains/models can handle the regularization better. More detailed analysis is required to explain this phenomenon.

Regularization (γ)	ResNet-18		VGG-19	
	Unlearning Error	Accuracy (%)	Unlearning Error	Accuracy (%)
0.0	132.49	77.11	141.73	77.69
1.0	101.79	74.5	123.17	76.81
5.0	98.3	73.21	113.27	77.16
10.0	90.71	69.13	107.9	74.07
15.0	86.17	68.46	78.82	65.32
20.0	11.5	34.74	27.94	31.18

Table 1: Unlearning error and testing accuracy on CIFAR-10 for a pretraining amount of 10 epochs.

⁴ $\gamma = 0$ means we just train with CE Loss (which acts as our baseline)

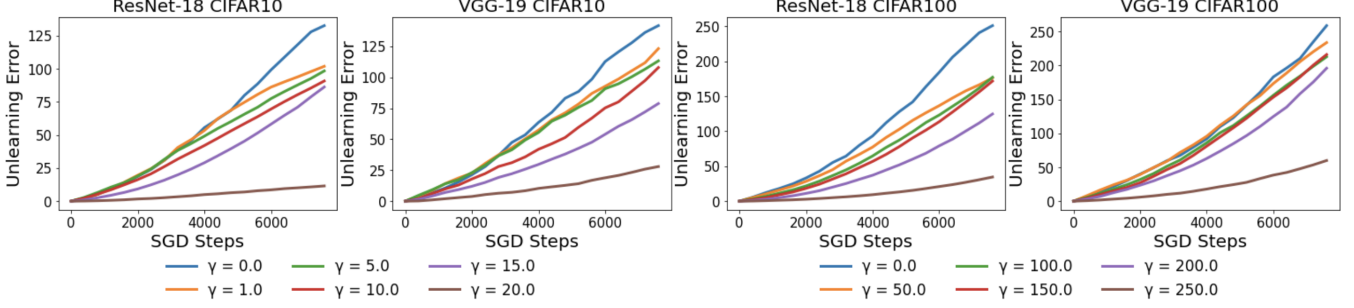


Figure 7: Unlearning error of 4 setups trained with the standard deviation loss with increasing levels of SD regularization. Across all 4 setups, a stronger regularization decreases the unlearning error at a (minimal) cost of the performance of the model.

Regularization (γ)	Unlearning Error	Verification Error	Test Accuracy (%)
0	85.10	4.35	92.13
0.01	85.89	4.27	92.53
0.1	71.73	3.43	92.38
0.5	31.98	1.57	92.71
1.0	8.91	0.57	92.09
1.25	5.60	0.43	87.22
1.5	2.57	0.48	84.99

Table 2: Unlearning error, verification error and testing accuracy for DistilBERT on the IMDB dataset for varying regularization amounts of the SD loss.

8.2 An Ablation Study

Recall that the unlearning error is dependent on t , σ_{avg} , \mathbf{w}_t , and also the value of N . As we can calculate the unlearning error with respect to different stages of training by varying the value of N , we can obtain a more nuanced view of how it evolves with respect to these factors. All results in this subsection are presented for the vision models only. The results are plotted for $N = 15625$ steps (10 epochs), and $t = 7812$ steps (5 epochs) in Figure 8, but the trends and ensuing discussion hold for all other values of N .

Singular Values & Change in Weights. The impact of SD loss on σ_{avg} and the final change in weights and largest singular values are presented in Figure 8 (left). We see that the impact to the singular values is *minimal*. After some initial oscillation, SD loss leaves σ_{avg} unchanged. Thus, the effect on reducing the unlearning error comes from elsewhere; we can see that SD loss *does decrease* the change in weights $\|\mathbf{w}_t - \mathbf{w}_0\|_2$ significantly with increasing γ^5 , as suggested by our analysis in § 6.2 (refer Figure 8 (right)). Recall that the change in weights influences the unlearning error, and smaller values of $\|\mathbf{w}_t - \mathbf{w}_0\|_2$ induces smaller values of e .

Influence of N . We wish to answer a more nuanced question: *how does the impact on SD loss vary as training progresses i.e., as N increases?* The results are presented in Table 4 in Appendix .3. We observe that as N increases, the decrease in unlearning error caused by a given regularization diminishes

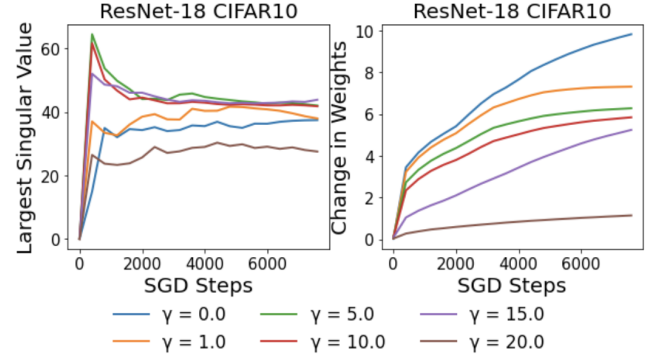


Figure 8: Largest singular value and change in weights over training for different regularization strengths for ResNet-18 on CIFAR-10. The change in weights decrease consistently and significantly as the regularization strength increases. (with the exception of ResNet-18 on CIFAR-10). Looking at VGG-19 on CIFAR-10 in Table 4, we see w.r.t the $N = 10$ epochs of pre-training row, $\gamma = 5$ decreases the unlearning error by 20% relative to the baseline ($\gamma = 0$). With respect to the $N = 30$ epochs of pre-training row, $\gamma = 5$ results in a 4% drop relative to the baseline ($\gamma = 0$). This reduced effect is due to the model converging (or being close to converging) to its final weights: recall that in our setup, the weights obtained after N steps of training are considered as \mathbf{w}_0 ; as N increases, the value of \mathbf{w}_t (which are the weights obtained after $N + t$ steps of training) are close to \mathbf{w}_0 .

8.3 Unlearning Error & Verification Error

Having established the relationship between unlearning error and SD loss, we wish to conclude our evaluation by validating if unlearning error is a good proxy for verification error. To this end, we evaluate the relationship between unlearning error and verification error with a specific emphasis on training duration t , regularization strength γ , and a combination of the two datasets and model architectures. For this experiment, we utilize the setup (and notation) from § 8.1 (i.e., both vision and text models) to compute unlearning error and the following setup to compute verification error:

⁵Here \mathbf{w}_t are the weights of the model M_{N+t} , and \mathbf{w}_0 of the model M_N .

1. Train M_N for $t - 1$ steps on batches $\hat{\mathbf{x}}_2, \dots, \hat{\mathbf{x}}_t$. The resulting model is the naively retrained model M' without batch $\hat{\mathbf{x}}_1$ (where note $\hat{\mathbf{x}}_1$ varies as we vary N) with weights \mathbf{w}' .
2. Obtain the approximately unlearned model M'' (in particular \mathbf{w}'') using our single gradient method as follows:

$$\mathbf{w}'' = \mathbf{w}_{N+t} + \frac{\eta}{b} \frac{\partial \mathcal{L}}{\partial \mathbf{w}} \bigg|_{\mathbf{w}_{N+t}, \hat{\mathbf{x}}_1}$$

where \mathbf{w}_{N+t} were the weights of M_{N+t} .

3. Compute the verification error (*i.e.*, $\|\mathbf{w}' - \mathbf{w}''\|_2$).

Changing t : In Figure 3 in § 6.1, we saw that unlearning error increases with t . To this end, we utilize the ResNet-18 model trained using CIFAR-10. We wish to understand if verification error also increases with t . Figure 9 (left) shows the relationship between the verification error and the unlearning error as a function of the number of steps t taken, for $t = 15625$ (5 epochs) steps after $N = 0$ steps. Observe that the two are strongly correlated (with a Pearson’s coefficient of 0.934). When we increase the value of N to 250000 steps (80 epochs) to measure how this effect is at a different stage of training (for the same value of t as before), we observe the same effect: there is a strong correlation between verification and unlearning error (with a Pearson’s coefficient of 0.9668); refer Figure 9 (right).

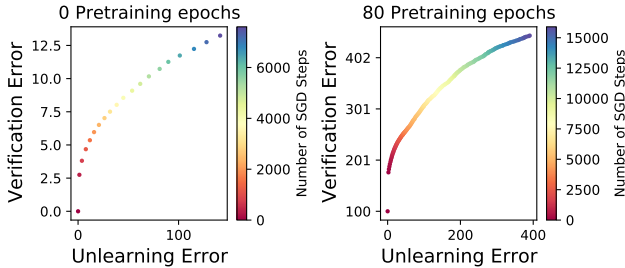


Figure 9: Unlearning error and verification error as a function of the fine-tuning steps (indicated by the color gradient) for ResNet-18 on CIFAR-10 for $N = 0$ steps (0 epochs), $t = 7812$ steps (5 epochs) and $N = 250000$ steps (80 epochs), $t = 15625$ (5 epochs). Unlearning error and verification error are measured every 400 and 100 SGD updates, respectively. The correlation between unlearning error and verification error as a function of t is 0.934 and 0.9668, respectively. Both unlearning error and verification error increase as a function of the number of fine-tuning steps.

Changing γ : Similarly, from Figure 11, we can observe that varying the strength of our regularization (γ) results in a strong correlation between unlearning error and the verification error. For ResNet-18 trained on CIFAR-10, the Pearson coefficient is 0.96, and the Pearson coefficient is 0.81 for VGG-19 trained

on CIFAR-10. Furthermore for DistilBERT fine-tuned on IMDB reviews we observe a Pearson Coefficient of 0.998 (see Figure 10). Also notice that for large values of γ (*i.e.*, the blue points near the origin), both verification and unlearning error are low. This further validates the efficacy of SD loss.

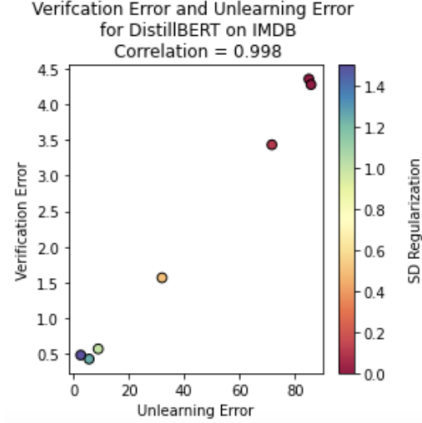


Figure 10: Correlation of verification error and unlearning error for DistilBERT on the IMDB dataset when varying the SD regularization strength.

Considering all models: The goal now is to see if unlearning error can be used to compare which architectures and training setups are better at unlearning (*i.e.*, does unlearning error strongly correlate with verification error across training setups). This is seen in Figure 12 where we consider 160 different training setups for CIFAR-10 and CIFAR-100⁶; we observe that generally when a model with a specific setup has lower unlearning error, it has lower verification error. This can be observed by looking at the strong positive correlation between unlearning error and the verification error across the different settings and architecture considered.

The fact that unlearning error is a good proxy for the verification error serves as evidence that the mathematical basis for unlearning error presented in § 5.2 holds for the different architectures, domains, and datasets we considered, despite the approximations we made to arrive at the definition of unlearning error. Another takeaway from this result, and the fact that the correlations stand across different architectures, is that unlearning error can be used to compare how well different models with potentially different architectures unlearn, leading to the possible study of what architectures unlearn better. We leave this aspect to future work.

9 Discussion

We focus on discussing open questions raised by our and others’ work.

⁶We consider different amounts of pre-training $N = \{10, 20, \dots, 80\}$ epochs, batch sizes $\{32, 64, 128\}$, SD regularization strengths (values between the ranges shown in Figure 7), models (ResNet-18 and VGG-19) and batch size over which the Hessian is calculated.

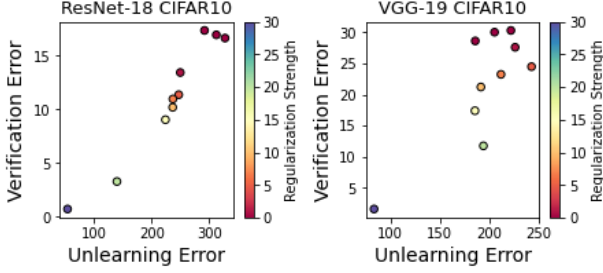


Figure 11: Correlation between unlearning error and verification error for ResNet-18 and VGG-19 on CIFAR-10 as a function of the regularization strength. The correlations are both high at 0.96 and 0.81 for ResNet-18 and VGG-19, respectively. Notice that the stronger the regularization (more blue) the more the verification and unlearning error decrease in both settings.

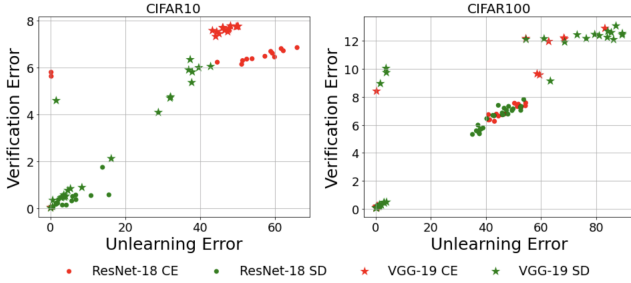


Figure 12: Unlearning and verification error for 160 settings across CIFAR-10 and CIFAR-100. The correlation between unlearning error and verification error for CIFAR-10 and CIFAR-100 are **0.9028** and **0.8813**, respectively. Settings trained with SD loss (green) for both datasets have lower unlearning and verification error than those trained with regular CE (red).

Experimental Constraints: We leverage the widely used implementation from [kuangliu](https://github.com/kuangliu/pytorch-cifar)⁷ which achieves a 93% test accuracy (on CIFAR-10) with ResNet18. We remove several enhancements, specifically:

1. Learning rate (η) scheduler: our derivation assumes a constant LR.
2. Data augmentation: introduces multiple copies of the unlearned data.
3. Momentum/ADAM: as our approximation was focused on SGD.

These restrictions are common when learning with differential privacy, and the drop to performance we experience on CIFAR-10 and CIFAR-100 is less significant. Nevertheless future work may be able to improve the performance

⁷<https://github.com/kuangliu/pytorch-cifar>

by utilising other enhancements or dropping some of these restrictions. It is worth noting however that DistilBERT was still able to achieve high test accuracy.

SISA Cost Comparison: An interesting question is whether exact unlearning could ever be cheaper than approximate unlearning. As our method is a very cheap form of approximate unlearning, and SISA is the cheapest exact unlearning method, we compare how the costs of exactly unlearning with SISA [7] compares to our approximate unlearning costs. The cost of unlearning with SISA is at best $\frac{2S}{(R+1)} \times \text{cost-to-retrain}$ [7] (R is number-of-slices and S is number-of-shards). Additionally, this requires $O(S.R)$ storage. Our cost is computing a single gradient (cost-to-retrain/ N where N is number-of-steps) and requires no storage. When $\frac{2S}{(R+1)} < \frac{1}{N}$ SISA could be faster, but then R or S is at least $\frac{\sqrt{N}}{2} - 1$ (and typically $N \approx 100,000$). Thus R and S would be significantly higher than what was originally tested by Bouroule *et al.*, and note that increasing S was observed to decrease performance, but future work may investigate training SISA with sufficiently large S and R .

Unlearning Error and Verification Error for other Unlearning Methods: An interesting question is whether our unlearning error serves as a good proxy for verification error even when employing unlearning methods besides our own. We focused on amnesiac machine learning [8], and computed the analogous result of Figure 12 in Figure 13 where we once again vary different batch sizes, training amounts, regularization strength(s), etc. except now M'' is obtained via amnesiac machine learning. As was the case for our approach, we see very strong correlations between unlearning error and verification error of 0.91 on CIFAR-10 and 0.81 on CIFAR-100. This begs the question of whether unlearning error can be used to assess the verification error (by proxy) of other approximate methods for unlearning in SGD. We leave this to future work.

Expanding Analysis of Verification Error: However, it should be noted that though amnesiac machine learning retains a strong correlation, it does not solely depend on \mathbf{w}_0 or I . This is because it computes gradients with respect to intermediate weights during training; training from the same \mathbf{w}_0 with the same batch ordering I , we get significantly different weights during the end of training. Thus, it violates the assumptions made by our analysis as it introduces significant noise we did not account for in our proofs. Thus the bounds presented in § 4 do not apply (*i.e.*, we are not sure if lowering verification error with these methods lowers the difference in probability distributions). However this does not mean similar bounds do not exist, and we leave it for future work to expand these results to other classes of unlearning methods and possibly expanding our existing assumptions on noise we used for the proofs.

Architectures and Unlearning Error: Recall from § 8.1, that the results of the ResNet architecture on CIFAR-10 were atypical. The SD loss on ResNet-18 continued to significantly

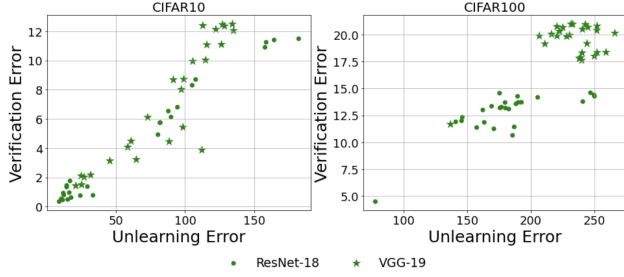


Figure 13: Unlearning and verification error for 104 settings across CIFAR-10 and CIFAR-100 using **amnesiac unlearning**. Correlations between unlearning error and verification error for CIFAR-10 and CIFAR-100 are resp. **0.91** and **0.81**.

reduce unlearning error into the later stages of training and in general dropped unlearning error with a smaller cost to performance compared to VGG-19; we also see from Table 4 that though SD loss effect diminishes for ResNet-18 on CIFAR-100, it is significantly less so than VGG-19. Similarly, DistilBERT in fact was able to drop unlearning error by a magnitude while seeing less significant drops to accuracy. This begs the question, are some models or domains just better for unlearning? We believe this is an interesting direction for future work to pinpoint what architectural or domain features make unlearning easier or harder.

Regularizers and Unlearning Error: Similarly future work might look into better regularizers, potentially ones focusing on reducing singular values, and improving the performance of our SD loss by a regularization scheduler that accounts for the degrading impact we noted in § 8.2.

10 Conclusion

In this paper we first discussed past work on approximate unlearning, noting how there was a great breadth to what metric one can use to define unlearning. Following this we showed how verification error captures a large class of unlearning metrics (under some assumptions), motivating using it to define an approximate unlearning method. However, as verification error cannot be optimized directly when devising an unlearning method (as it requires a perfectly unlearned model for computation), we decomposed SGD with a Taylor series to first propose our single-gradient unlearning method, and furthermore propose our *unlearning error* which we showed effectively proxies verification error when using our unlearning method. To then improve the effectiveness of our unlearning approach, we looked at the variables our proxy metric depends on and proposed our SD loss which we showed can effectively decrease the unlearning error (and thus the verification error) associated with our unlearning method. We expect that future work will try and improve the loss we used in our work, or see how it may help with dif-

ferent machine learning related tasks, and extend the bounds we presented in our work to other contexts and see if certain assumptions can be dropped.

References

- [1] R. Shokri, M. Stronati, C. Song, and V. Shmatikov, "Membership inference attacks against machine learning models," in *2017 IEEE Symposium on Security and Privacy (SP)*. IEEE, 2017, pp. 3–18.
- [2] M. Abadi, A. Chu, I. Goodfellow, H. B. McMahan, I. Mironov, K. Talwar, and L. Zhang, "Deep learning with differential privacy," in *Proceedings of the 2016 ACM SIGSAC conference on computer and communications security*, 2016, pp. 308–318.
- [3] A. Mantelero, "The eu proposal for a general data protection regulation and the roots of the 'right to be forgotten'," *Computer Law & Security Review*, vol. 29, no. 3, pp. 229–235, 2013.
- [4] N. Carlini, C. Liu, Ú. Erlingsson, J. Kos, and D. Song, "The secret sharer: Evaluating and testing unintended memorization in neural networks," in *28th {USENIX} Security Symposium ({USENIX} Security 19)*, 2019, pp. 267–284.
- [5] M. Fredrikson, S. Jha, and T. Ristenpart, "Model inversion attacks that exploit confidence information and basic countermeasures," in *Proceedings of the 22nd ACM SIGSAC Conference on Computer and Communications Security*, 2015, pp. 1322–1333.
- [6] Y. Cao and J. Yang, "Towards making systems forget with machine unlearning," in *2015 IEEE Symposium on Security and Privacy*. IEEE, 2015, pp. 463–480.
- [7] L. Bourtole, V. Chandrasekaran, C. A. Choquette-Choo, H. Jia, A. Travers, B. Zhang, D. Lie, and N. Papernot, "Machine unlearning," *arXiv preprint arXiv:1912.03817*, 2019.
- [8] L. Graves, V. Nagisetty, and V. Ganesh, "Amnesiac machine learning," *arXiv preprint arXiv:2010.10981*, 2020.
- [9] A. Golatkar, A. Achille, and S. Soatto, "Eternal sunshine of the spotless net: Selective forgetting in deep networks," in *Proceedings of the IEEE/CVF Conference on Computer Vision and Pattern Recognition*, 2020, pp. 9304–9312.
- [10] A. Sekhari, J. Acharya, G. Kamath, and A. T. Suresh, "Remember what you want to forget: Algorithms for machine unlearning," *arXiv preprint arXiv:2103.03279*, 2021.
- [11] C. Guo, T. Goldstein, A. Hannun, and L. Van Der Maaten, "Certified data removal from machine learning models," *arXiv preprint arXiv:1911.03030*, 2019.
- [12] T. Baumhauer, P. Schöttle, and M. Zeppelzauer, "Machine unlearning: Linear filtration for logit-based classifiers," *arXiv preprint arXiv:2002.02730*, 2020.
- [13] A. Golatkar, A. Achille, and S. Soatto, "Forgetting outside the box: Scrubbing deep networks of information accessible from input-output observations," *CoRR*, vol. abs/2003.02960, 2020. [Online]. Available: <https://arxiv.org/abs/2003.02960>
- [14] T. Hastie, R. Tibshirani, and J. Friedman, "Overview of supervised learning," in *The elements of statistical learning*. Springer, 2009, pp. 9–41.
- [15] A. Krizhevsky, I. Sutskever, and G. E. Hinton, "Imagenet classification with deep convolutional neural networks," *Advances in neural information processing systems*, vol. 25, pp. 1097–1105, 2012.
- [16] D. R. Cox, "The regression analysis of binary sequences," *Journal of the Royal Statistical Society: Series B (Methodological)*, vol. 20, no. 2, pp. 215–232, 1958.
- [17] J. Kiefer, J. Wolfowitz *et al.*, "Stochastic estimation of the maximum of a regression function," *The Annals of Mathematical Statistics*, vol. 23, no. 3, pp. 462–466, 1952.
- [18] T. B. Brown, B. Mann, N. Ryder, M. Subbiah, J. Kaplan, P. Dhariwal, A. Neelakantan, P. Shyam, G. Sastry, A. Askell *et al.*, "Language models are few-shot learners," *arXiv preprint arXiv:2005.14165*, 2020.
- [19] Y. Wu, E. Dobriban, and S. B. Davidson, "Deltagrad: Rapid retraining of machine learning models," 2020.
- [20] H. Jia, M. Yaghini, C. A. Choquette-Choo, N. Dullerud, A. Thudi, V. Chandrasekaran, and N. Papernot, "Proof-of-learning: Definitions and practice," *arXiv preprint arXiv:2103.05633*, 2021.
- [21] C. Dwork, A. Roth *et al.*, "The algorithmic foundations of differential privacy," *Foundations and Trends in Theoretical Computer Science*, vol. 9, no. 3-4, pp. 211–407, 2014.
- [22] V. Gupta, C. Jung, S. Neel, A. Roth, S. Sharifi-Malvajerdi, and C. Waites, "Adaptive machine unlearning," *arXiv preprint arXiv:2106.04378*, 2021.
- [23] B. W. Jimmy Ba, "Csc421/2516 lecture 3: Automatic differentiation & distributed representations," Lecture Notes, WS 2021.
- [24] L. Song and P. Mittal, "Systematic evaluation of privacy risks of machine learning models," in *30th {USENIX} Security Symposium ({USENIX} Security 21)*, 2021.

- [25] S. Yeom, I. Giacomelli, M. Fredrikson, and S. Jha, “Privacy risk in machine learning: Analyzing the connection to overfitting,” in *2018 IEEE 31st Computer Security Foundations Symposium (CSF)*. IEEE, 2018, pp. 268–282.
- [26] A. Krizhevsky *et al.*, “Learning multiple layers of features from tiny images,” *Master’s Thesis*, 2009.
- [27] K. He, X. Zhang, S. Ren, and J. Sun, “Deep residual learning for image recognition,” *CoRR*, vol. abs/1512.03385, 2015. [Online]. Available: <http://arxiv.org/abs/1512.03385>
- [28] K. Simonyan and A. Zisserman, “Very deep convolutional networks for large-scale image recognition,” *arXiv preprint arXiv:1409.1556*, 2014.
- [29] A. Browder, *Mathematical analysis: an introduction*. Springer Science & Business Media, 2012.
- [30] B. A. Pearlmutter, “Fast exact multiplication by the hessian,” *Neural computation*, vol. 6, no. 1, pp. 147–160, 1994.
- [31] V. Sanh, L. Debut, J. Chaumond, and T. Wolf, “Distilbert, a distilled version of bert: smaller, faster, cheaper and lighter,” *arXiv preprint arXiv:1910.01108*, 2019.
- [32] A. Maas, R. E. Daly, P. T. Pham, D. Huang, A. Y. Ng, and C. Potts, “Learning word vectors for sentiment analysis,” in *Proceedings of the 49th annual meeting of the association for computational linguistics: Human language technologies*, 2011, pp. 142–150.

1 Proofs

Approximation to Bounded Domain of positive $L^1(\mathbb{R})$ Functions If $F(x)$ is a positive $L^1(\mathbb{R})$ function (for example a probability density function), define $F_n(x)$ as the restriction of $F(x)$ to $[-n, n]$. Note then $F_n(x)$ converges to F pointwise, and $F_n \leq F$. Thus by dominated convergence we have $\lim_n \int_{[-n, n]} F_n(x) = \int_{\mathbb{R}} F(x)$, i.e., $\forall \epsilon \geq 0$ there $\exists n$ s.t. $\int_{\mathbb{R}} F(x) - F_n(x) \leq \epsilon$ and note $F_n(x)$ has bounded domain.

Lemma 1

We have:

$$\begin{aligned}
& \|\mathbb{P}(\mathbf{w}) - \mathbb{P}'(\mathbf{w})\|_2 = \\
& \|\mathbb{P}(\mathbf{w}) - \mathbb{P}'(\mathbf{w}) + \frac{(n-1)!^m}{n!^m} (n^m \mathbb{P}'(\mathbf{w}) - n^m \mathbb{P}'(\mathbf{w}))\|_2 \\
& \leq \left\| \frac{1}{n!^m} \sum_I \mathbb{P}_I(\mathbf{w}) - \mathbb{P}'_I(\mathbf{w}) \right\|_2 + \left| \left(\frac{(n-1)!^m n^m}{n!^m} - 1 \right) \right| \|\mathbb{P}'(\mathbf{w})\|_2 \\
& \leq \frac{1}{n!^m} \sum_I \|\mathbb{P}_I(\mathbf{w}) - \mathbb{P}_I(\mathbf{w} - \mathbf{d}_I)\|_2 \quad (13)
\end{aligned}$$

Where the step from the first line to the second line follows from noting that by having n^m copies of $(n-1)!^m \mathbb{P}'(\mathbf{w}) = \sum_{I'} \mathbb{P}'_{I'}(\mathbf{w})$ we can associate to each $\mathbb{P}_I(\mathbf{w})$ its corresponding $\mathbb{P}'_{I'}(\mathbf{w})$, which comes from the previous remark on counting of I and I' . If we assume every \mathbb{P}_I is lipschitz (which is true for Gaussian noise), then $\|\mathbb{P}_I(\mathbf{w}) - \mathbb{P}_I(\mathbf{w} - \mathbf{d}_I)\|_2 \leq L_I \|\mathbf{d}_I\|_2$; note by definition all \mathbb{P}_I are just the same distributions but shifted (as we have the same noise \mathbf{g} for each plus some varying constant \mathbf{w}_I), thus all the L_I are equal, i.e., $L_I = L$ for every I (as translating a function doesn’t change its lipschitz constant). Lastly if we let d be the average of all the \mathbf{d}_I , that is $d = \frac{1}{n!^m} \sum_I \|\mathbf{d}_I\|_2$, we have

$$\|\mathbb{P}(\mathbf{w}) - \mathbb{P}'(\mathbf{w})\|_2 \leq Ld \quad (14)$$

which gives a uniform bound on the l2 difference of $\mathbb{P}(\mathbf{w})$ and $\mathbb{P}'(\mathbf{w})$.

Corollary 1

To understand how this relates to verification error and approximate unlearning, let us consider an approximate unlearning method which only looks at \mathbf{w}_0 and I and to \mathbf{w}_I obtains the approximately unlearned weights $\mathbf{w}_I'' = \mathbf{w}_I + \mathbf{u}_I$ where \mathbf{u}_I is some unlearning update. Note then we can analogously define a $\mathbf{z}_I'' = \mathbf{w}_I + \mathbf{u}_I + \mathbf{g}$ as before with corresponding density function $\mathbb{P}_I''(\mathbf{w})$. Defining $\mathbf{v}_I = \mathbf{u}_I + \mathbf{d}_I$ we get $\mathbf{z}_I'' = \mathbf{z}_I' - \mathbf{v}_I$ where \mathbf{v}_I represents the analytic (ignoring noise) verification error for the given ordering I (i.e., the difference between the weights obtained from the approximate unlearning \mathbf{w}_I'' and the retrained weights \mathbf{w}_I). At this point it is clear all the previous steps follow and defining v as the average of all the $\|\mathbf{v}_I\|_2$ we get

$$\|\mathbb{P}''(\mathbf{w}) - \mathbb{P}'(\mathbf{w})\|_2 \leq Lv \quad (15)$$

where now $\mathbb{P}''(\mathbf{w}) = \frac{1}{n!^m} \sum_I \mathbb{P}_I''$ represents the probability density function of the weights after applying the approximate unlearning method on M to obtain M'' . **Reverse Direction of Corollary 1** We now proceed to get a bound on the average verification error v based on a uniform bound between the density function after the approximate unlearning and the density function for ideal retraining.

Note, assuming the noise has 0 mean, v is simply the difference in expectation of $\mathbb{P}''(\mathbf{w})$ and $\mathbb{P}'(\mathbf{w})$, and let us for the time being assume that the union of the support of $\mathbb{P}''(\mathbf{w})$ and $\mathbb{P}'(\mathbf{w})$ is bounded, i.e., if \mathbf{W} is the union of the supports, then $\int_{\mathbf{W}} \|\mathbf{w}\|_2 d\mathbf{w} = a < \infty$. This is reasonable as we would expect the noise from training to be bounded; in fact in general we would only need the integral outside a bounded domain to be finite, but the reasoning is analogous to what follows and would simply add an extra constant term. Now if say $\|\mathbb{P}''(\mathbf{w}) - \mathbb{P}'(\mathbf{w})\|_2 < b$ for some scalar b for all w (i.e., b is a

uniform bound), we have:

$$\begin{aligned}
v &= \|\mathbb{E}(\mathbb{P}''(\mathbf{w})) - \mathbb{E}(\mathbb{P}'(\mathbf{w}))\|_2 \\
&= \left\| \int_{\mathbf{w}} \mathbb{P}''(\mathbf{w}) \mathbf{w} d\mathbf{w} - \int_{\mathbf{w}} \mathbb{P}'(\mathbf{w}) \mathbf{w} d\mathbf{w} \right\|_2 \\
&\leq \int_{\mathbf{w}} \|\mathbb{P}''(\mathbf{w}) - \mathbb{P}'(\mathbf{w})\|_2 \cdot \|\mathbf{w}\|_2 d\mathbf{w} \\
&\leq ba \quad (16)
\end{aligned}$$

and so in this sense we see reducing the max value of $\|\mathbb{P}(\mathbf{w}) - \mathbb{P}'(\mathbf{w})\|_2$ gives a smaller bound on the expectation of verification error v .

2 Additional Figures

In Figure 14, the change in weights and singular values for varying strengths of the ℓ_2 regularization is shown. Figure 15 and 13 are identical setups to Figure 9 and 12 but using amnesiac unlearning to produce the model M'' .

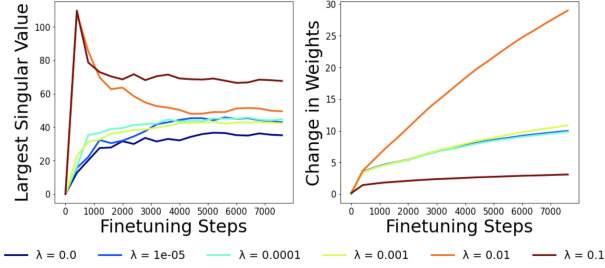


Figure 14: Change in weights and singular values during training for different strengths of ℓ_2 regularization for ResNet-18 trained on CIFAR-10

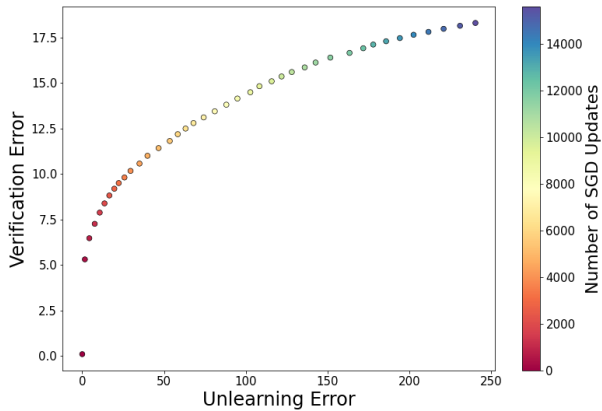


Figure 15: Unlearning error and verification error as a function of the finetuning steps (indicated by the color gradient) for ResNet-18 on CIFAR-10 using **amnesiac unlearning**

3 Additional Tables

In Table 3, the unlearning error and test accuracy for the 4 setups as a function of the ℓ_2 regularization strength and pretraining amount (in epochs) are shown. Table 4 shows a similar experiment but with the proposed SD regularization.

Pretrain Epochs	Regularization CIFAR-10	ResNet-18 CIFAR-10		VGG-19 CIFAR-10		Regularization CIFAR-100	ResNet-18 CIFAR-100		VGG-19 CIFAR-100	
		Unlearning Error	Accuracy (%)	Unlearning Error	Accuracy (%)		Unlearning Error	Accuracy (%)	Unlearning Error	Accuracy (%)
0	0.0	148.31	10.84	200.66	10.2	0.0	154.51	0.95	359.05	1.18
	1e-05	145.44	10.68	174.23	10.87	1e-05	171.82	0.94	256.09	1.12
	0.0001	164.48	8.78	165.01	10.53	0.0001	159.26	1.22	501.29	0.92
	0.001	613.22	9.65	199.99	9.85	0.001	161.26	0.85	547.47	0.98
	0.01	702.94	9.54	772.91	10.01	0.01	651.45	1.18	1162.51	1.0
	0.1	2092.77	10.43	3980.42	10.52	0.1	854.97	1.11	3211.49	1.08
20	0.0	161.09	76.61	108.75	79.14	0.0	182.06	45.71	214.51	51.71
	1e-05	174.62	75.98	116.3	79.98	1e-05	174.36	46.69	201.91	52.07
	0.0001	142.46	76.94	141.75	79.51	0.0001	191.54	46.53	206.77	51.78
	0.001	205.24	76.11	137.72	80.24	0.001	171.26	47.29	214.15	52.35
	0.01	421.03	67.73	346.64	79.93	0.01	458.96	49.53	361.27	55.18
	0.1	86.73	77.95	176.45	80.85	0.1	–	7.0	383.14	24.72
40	0.0	152.67	76.94	106.7	81.71	0.0	169.7	44.68	214.5	51.4
	1e-05	176.08	76.71	111.17	82.5	1e-05	177.19	45.36	221.92	51.74
	0.0001	162.47	76.13	–	–	0.0001	201.82	45.89	225.43	52.91
	0.001	159.88	76.18	122.83	82.48	0.001	235.74	46.37	228.98	53.58
	0.01	189.76	71.75	224.72	80.93	0.01	265.38	45.76	271.12	60.22
	0.1	101.32	81.28	182.46	75.73	0.1	361.16	5.4	290.84	20.5

Table 3: Unlearning error and testing accuracy for 4 different settings for varying regularization strengths of the ℓ_2 regularizer and pretraining amount compared to zero regularization.

Pretrain Epochs	Regularization CIFAR-10	ResNet-18 CIFAR-10		VGG-19 CIFAR-10		Regularization CIFAR-100	ResNet-18 CIFAR-100		VGG-19 CIFAR-100	
		Unlearning Error	Accuracy (%)	Unlearning Error	Accuracy (%)		Unlearning Error	Accuracy (%)	Unlearning Error	Accuracy (%)
0	0.0	141.35	8.82	160.95	9.03	0.0	165.65	0.78	245.66	1.09
	1.0	110.32	9.66	348.85	10.51	50.0	142.59	1.01	381.88	1.38
	5.0	102.71	9.82	139.47	9.98	100.0	127.31	0.99	288.04	1.0
	10.0	90.66	10.06	203.44	10.15	150.0	110.48	0.95	186.17	1.0
	15.0	44.85	10.61	156.59	10.07	200.0	58.59	0.74	48.08	0.85
	20.0	21.63	10.32	69.34	9.5	250.0	30.81	0.85	34.56	1.21
10	0.0	132.49	77.11	141.73	77.69	0.0	251.12	44.07	258.63	48.39
	1.0	101.79	74.5	123.17	76.81	50.0	176.35	43.52	233.65	50.08
	5.0	98.3	73.21	113.27	77.16	100.0	177.28	43.12	212.71	47.49
	10.0	90.71	69.13	107.9	74.07	150.0	171.77	38.5	216.0	46.97
	15.0	86.17	68.46	78.82	65.32	200.0	124.74	26.68	195.89	36.75
	20.0	11.5	34.74	27.94	31.18	250.0	34.53	13.76	59.9	8.98
20	0.0	153.78	76.34	120.19	79.05	0.0	194.65	45.79	260.59	52.27
	1.0	109.07	74.14	135.44	80.93	50.0	140.1	45.77	220.46	52.55
	5.0	90.61	74.01	93.58	79.97	100.0	165.91	45.45	208.58	53.12
	10.0	86.31	69.88	100.09	78.21	150.0	181.78	44.89	233.99	52.42
	15.0	86.67	68.69	95.62	73.81	200.0	184.81	41.18	241.61	47.34
	20.0	10.74	36.29	32.23	38.88	250.0	116.28	27.7	131.24	23.15
30	0.0	153.26	76.48	113.37	81.5	0.0	210.35	45.68	250.87	52.17
	1.0	112.01	73.7	130.25	81.18	50.0	151.56	45.02	194.86	52.69
	5.0	94.44	72.48	108.84	80.24	100.0	178.74	45.57	229.36	52.88
	10.0	83.53	70.19	116.96	78.76	150.0	205.75	42.71	217.5	52.48
	15.0	88.96	69.17	92.93	77.13	200.0	203.18	43.1	256.51	51.81
	20.0	13.73	36.98	49.03	48.69	250.0	127.97	28.52	200.4	37.02
40	0.0	175.32	75.59	120.92	82.07	0.0	209.52	45.11	219.14	52.32
	1.0	97.11	74.86	109.44	80.89	50.0	176.31	45.45	250.64	52.36
	5.0	93.74	73.58	108.54	80.21	100.0	201.74	45.01	251.3	53.01
	10.0	83.11	70.33	92.38	79.31	150.0	211.01	42.12	233.39	52.49
	15.0	79.86	68.7	96.14	77.64	200.0	218.61	41.58	233.58	50.67
	20.0	8.24	41.02	58.35	44.14	250.0	198.57	41.05	253.88	45.69
50	0.0	184.99	76.89	118.56	81.39	0.0	235.23	45.51	221.19	52.47
	1.0	100.39	74.51	121.06	81.37	50.0	168.65	44.91	226.56	51.95
	5.0	88.43	73.57	114.11	80.31	100.0	206.35	44.57	224.88	52.67
	10.0	80.72	72.14	113.41	79.28	150.0	229.16	43.73	230.4	53.57
	15.0	76.42	71.39	87.12	77.17	200.0	234.73	43.04	255.56	51.29
	20.0	17.43	37.31	77.01	68.4	250.0	228.22	40.7	254.52	47.52

Table 4: Unlearning error and testing accuracy for 4 different settings for varying regularization strengths of the Standard Deviation regularizer and pretraining amount.